Title
Power performance of AlGaN-GaNHEMTs grown on SiC by plasma-assisted MBE

Journal
IEEE Electron Device Letters, 25(5)

ISSN
0741-3106

Authors
Rajan, Siddharth
Waltereit, P
Poblenz, C
et al.

Publication Date
2004-05-01

Peer reviewed

Power Performance of AlGaN–GaN HEMTs Grown on SiC by Plasma-Assisted MBE

Siddharth Rajan, Patrick Waltereit, Christiane Poblenz, Sten J. Heikman, Daniel S. Green, James S. Speck, and Umesh K. Mishra, *Fellow, IEEE*

***Abstract*—We report AlGaN–GaN high electron mobility transistors (HEMTs) grown by molecular beam epitaxy (MBE) on SiC substrates with excellent microwave power and efficiency performance. The GaN buffers in these samples were doped with carbon to make them insulating. To reduce gate leakage, a thin silicon nitride film was deposited on the AlGaN surface by chemical vapor deposition. At 4 GHz, an output power density of 6.6 W/mm was obtained with 57% power-added efficiency (PAE) and a gain of 10 dB at a drain bias of 35 V. This is the highest PAE reported until now at 4 GHz in AlGaN–GaN HEMTs grown by MBE. At 10 GHz, we measured an output power density of 7.3 W/mm with a PAE of 36% and gain of 7.6 dB at 40-V drain bias.**

***Index Terms*—Carbon, gallium nitride, high electron mobility transistor (HEMT), microwave power, molecular beam epitaxy (MBE), power-added efficiency (PAE), silicon nitride.**

I. Introduction

In THE PAST few years, advances in materials and device technology have led to greatly improved performance from AlGaN–GaN HEMTs. These devices are promising for microwave power applications due to the high breakdown field and high electron velocity in GaN and because large electron concentrations can be obtained in the channel.

AlGaN–GaN HEMT devices with good RF performance have been fabricated on material grown by both metal–organic chemical vapor deposition (MOCVD) [1]–[4] and molecular beam epitaxy (MBE) [5]–[8] growth techniques. The advantages of MBE growth include high uniformity, *in situ* monitoring, and sharp interfaces. However, undoped GaN buffers grown by MBE are not always insulating, and this buffer leakage leads to degradation of transistor performance. To solve this problem, the HEMT buffers in this work are doped with carbon, which acts as a compensating acceptor and makes the reduces buffer conductivity. This is analogous to the use of iron in MOCVD grown HEMT buffers [9].

GaN transistors grown directly on SiC substrates by MBE also tend to have a higher gate leakage than MOCVD-grown transistors, possibly due to the higher dislocation density in MBE-grown material. In the past, silicon nitride (SiN_X) layers have been used under the gate to reduce gate leakage in GaN-based devices [10], [11]. In this letter, we use a thin insulating SiN_X film grown by high-temperature chemical vapor deposition (CVD) [12]. The use of SiN_X reduces gate leakage by an order of magnitude, and hence, improves breakdown voltage and device reliability.

The optimization of growth, introduction of carbon doping, and the use of an insulating silicon nitride layer have helped us achieve record power densities (>7 W/mm) at 10 GHz using 0.7 μm gate-length devices. We achieved record power-added efficiency(PAE) values for MBE-based HEMTs of 57% PAE with an output power of 6.6 W/mm at 4 GHz.

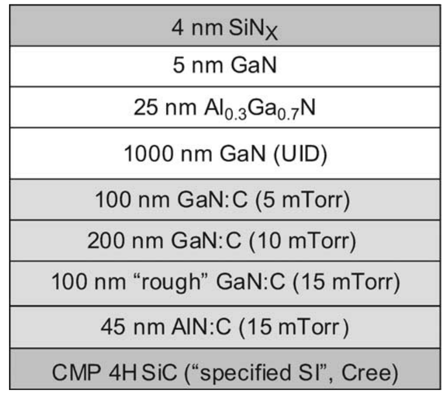

Fig. 1. Epitaxial structure of HEMTs discussed in this work. The epi-structure was grown by MBE, while the 4-nm silicon nitride cap was grown by high-temperature CVD. The carbon-doped regions are labeled with the pressure in the carbon source. See text for estimates of carbon concentration.

II. Growth and Device Processing

The HEMT structures described in this work were grown by plasma-assisted MBE on specified semi-insulating 4H-SiC (Cree). Fig. 1 shows the epitaxial structure of the device described here. A commercial CBr_4 gas source was used for carbon-doping the buffers [13]. A 45-nm-thick AlN:C nucleation layer was grown with a CBr_4 pressure of 15 mTorr in the source. This same CBr_4 pressure was used in the next 100 nm of GaN:C. From secondary ion mass spectrometry (SIMS) measurements the carbon concentration in the GaN for these conditions was found to be 1.2×10^{18} cm^{-3}. A two-step buffer approach was developed to grow the GaN buffers [14], [15]. The first GaN layer was grown in the intermediate Ga-flux regime [16] to help reduce threading dislocations in the material. The next 300 nm of GaN:C were grown in the high Ga-flux regime, with C-doping concentration (estimated

Manuscript received December 1, 2003; revised February 12, 2004. This work was supported in part by Defense Advanced Research Projects Agency, the Office of Naval Research, the Air Force Office of Scientific Research, and the California Nanoscience Innovation for Defense program.

S. Rajan, S. J. Heikman, and U. K. Mishra are with the Electrical and Computer Engineering Department, University of California, Santa Barbara, CA 93106 USA (e-mail: srajan@ece.ucsb.edu). The review of this letter was arranged by Editor D. Ritter.

P. Waltereit, C. Poblenz, and J. S. Speck are with the Materials Department, University of California, Santa Barbara, CA 93106 USA.

D. S. Green is with RF Micro Devices, Charlotte, NC 28269 USA.

Digital Object Identifier 10.1109/LED.2004.826977

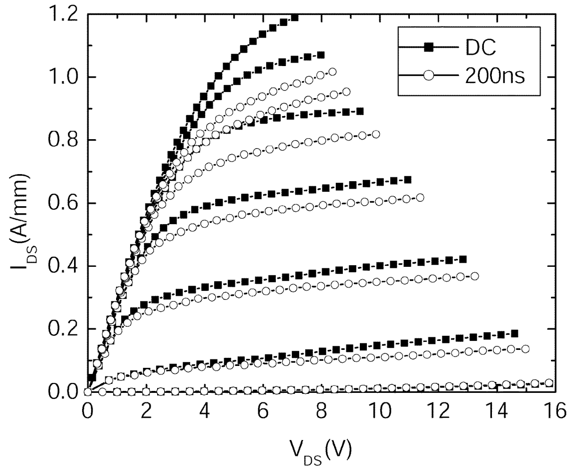

Fig. 2. DC and 200-ns current–voltage curves of the HEMT. The gate voltage was varied between -10 V and $+2$ V in steps of 2 V.

from SIMS) of 8×10^{17} cm^{-3} in the first 200 nm of material, and 4×10^{17} cm^{-3} in the last 100 nm. This was followed by 1 μm of undoped GaN grown in the high Ga-flux regime. A 25-nm-thick 30% AlGaN cap was grown on top of this structure, followed by a 5–nm UID GaN cap.

To reduce gate leakage, a 4-nm-thick SiN cap was deposited on top of the sample by high-temperature CVD [12]. Standard processing steps were employed to fabricate the transistors. Ti–Al–Ni–Au ohmic contacts were evaporated using e-beam deposition, and the contacts were alloyed by annealing for 30 s at 870 °C. This was followed by a BCl_3/Cl_2 reactive ion etch for mesa isolation, and Ni–Au–Ni gate metal evaporation. Finally, the surface was passivated with silicon nitride deposited by plasma enhanced CVD at 250 °C and contacts were made to the gate, source/drain pads by etching the passivating silicon nitride in CF_4 plasma. The 150-μm–wide devices had a gate length of 0.7 μm and a source/drain distance of 3.4 μm.

III. Results and Discussion

The dc and 200-ns pulsed output characteristics of the device are shown in Fig. 2. The gate voltage was varied from -10 V to $+2$ V in steps of 2 V. For the 200-ns pulsed measurements, the gate was pulsed with the device biased on a 50 Ω load-line. The maximum current was 1.2 A/mm, and the pinch-off voltage was -10 V. The transconductance of this device was 150 mS/mm at a drain bias of 10 V.

As shown in Fig. 2, the 200-ns pulsed current values were lower than the corresponding dc values. We observed that the currents measured using longer 80 μs pulses were the same as the 200-ns pulsed currents. Also, RF current–voltage (*I–V*) curves measured using a microwave transition analyzer showed no further current collapse at 4 GHz. This suggests that there is little or no reduction in the current response of the device as time scales are lowered from 200 ns to microwave periods. Further studies to characterize the dispersion due to carbon in the buffer are underway.

The three-terminal breakdown voltage was found to be greater than 100 V after passivation. The SiN_X cap reduced

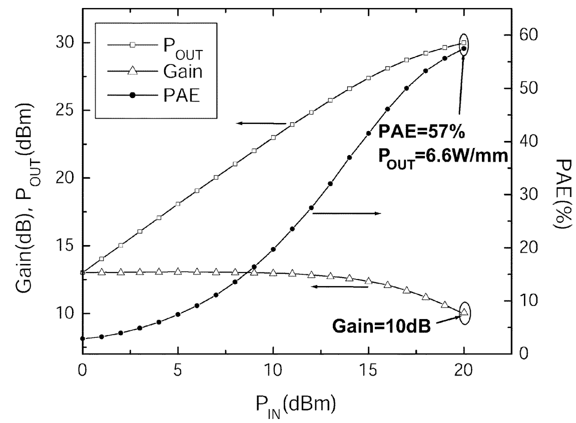

Fig. 3. Load-pull measurements at 4 GHz. The device was biased with $V_{\rm DS} = 35$ V and $I_{\rm DS} = 130$ mA/mm.

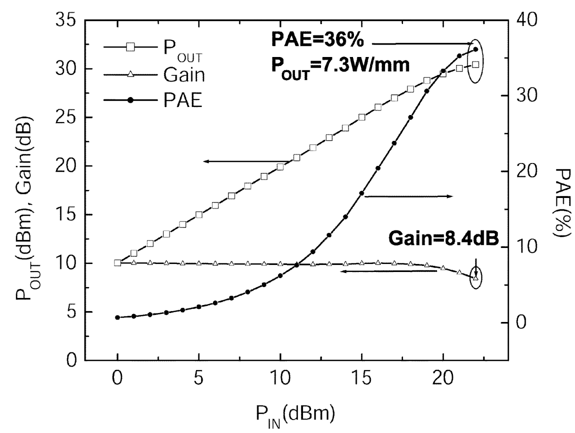

Fig. 4. Load-pull measurements at 10 GHz. The device was biased with $V_{\rm DS} = 35$ V and $I_{\rm DS} = 200$ mA/mm.

gate leakage by an order of magnitude and hence improved the gate-drain breakdown characteristics.

Small-signal measurements were carried out on the device. The current gain h_{21}, and the unilateral power gain were calculated from the measured *S*-parameters. Linear extrapolation of the current and power gain along a 20-dB/dec slope led to values of 21 and 46 GHz for the current gain cutoff frequency, f_τ, and the maximum oscillation frequency, $f_{\rm MAX}$, respectively. The bias conditions were $V_{\rm DS} = 15$ V and $I_{\rm DS} = 380$ mA/mm.

In Fig. 3, load-pull measurement results at 4 GHz are shown for a drain bias of 35 V. An output power density of 6.6 W/mm, a PAE of 57% anda gain of 10 dB were obtained with the gate biased at -8.1 V. At a drain bias of 30 V, the output power was 5.4 W/mm, with a PAE of 60% and 9 dB of gain. To our knowledge, these are the highest reported PAE values at 4 GHz for MBE-grown AlGaN–GaN HEMTs. The previous highest reported value for PAE from MBE-grown transistors [8] is 49% at 2 GHz with an output power density of 6.6 W/mm.

Load-pull power measurements were carried out at 10 GHz, and the results for a drain bias of 40 V are shown in Fig. 4. An output power density of 7.3 W/mm with a PAE of 36% and a gain of 8.4 dB was obtained at a drain bias of 40 V. This output power is highest reported at 10 GHz from MBE-grown HEMTs. The same device gave an output power of 6.1 W/mm with a PAE of 38% and a gain of 7.6 dB at a drain bias of 35 V. The drain efficiency was 42% and 46% at 40 and 35 V, respectively.

IV. Conclusion

We have demonstrated MBE-grown AlGaN–GaN HEMT structures with high output power density and record PAE among MBE-grown HEMTs. The efficiency and power results from these devices are comparable to the best MOCVD-grown HEMT results. For a 10 GHz continuous wave input signal, we obtained an output power density of 7.3 W/mm, with a PAE of 36% and output gain of 7.6 dB at a drain bias of 40 V. At 4 GHz, we obtained 6.6 W/mm, with a PAE of 57% and output gain of 10 dB at a drain bias of 35 V. Carbon doping is used to make highly insulating buffers reliably and reproducibly. Gate leakage in MBE-grown structures is reduced considerably by using a thin SiN layer below the gate.

Acknowledgment

The authors would like to thank T. Mates for SIMS measurements, and R. Coffie, L. Shen, and A. Chini for helpful discussions.

References

[1] A. Zhang, L. B. Rowland, E. B. Kaminsky, J. B. Tucker, J. W. Kretchmer, A. F. Allen, J. Cook, and B. J. Edward, "9.2 W/mm (13.8 W) AlGaN–GaN HEMTs at 10 GHz and 55 V drain bias," *Electron. Lett.*, vol. 39, pp. 245–247, 2003.

[2] L. Shen, R. Coffie, D. Buttari, S. Heikman, A. Chakraborty, A. Chini, S. Keller, S. P. DenBaars, and U. K. Mishra, "High-power polarization engineered GaN–AlGaN–GaN HEMTs without surface passivation," IEEE Electron Device Lett., vol. 25, May 2004, to be published.

[3] C. Lee, P. Saunier, J. Yang, and M. Khan, "AlGaN-GaN HEMTs on SiC with CW power performance of >4 W/mm and 23% PAE at 35 GHz," *IEEE Electron Device Lett.*, vol. 24, pp. 616–618, Oct. 2003.

[4] J. R. Shealy, V. Kaper, V. Tilak, T. Prunty, J. A. Smart, B. Green, and L. F. Eastman, "An AlGaN–GaN high-electron-mobility transistor with an AlN sub-buffer layer," *Phys. Rev. B, Condens. Matter*, vol. 14, pp. 3499–3509, 2002.

[5] J. S. Moon, M. Micovic, P. Janke, P. Hashimoto, W.-S. Wong, R. D. Widman, L. McCray, A. Kurdoghlian, and C. Nguyen, "GaN–AlGaN HEMTs operating at 20 GHz with a continuous-wave power density >6 W/mm," *Electron. Lett.*, vol. 37, pp. 528–530, 2001.

[6] D. S. Katzer, S. C. Binari, D. F. Storm, J. A. Roussos, B. V. Shanabrook, and E. R. Glaser, "MBE growth of AlGaN–GaN HEMTs with high power density," *Electron. Lett.*, vol. 38, pp. 1740–1741, 2002.

[7] N. G. Weimann, M. J. Manfra, and T. Wächtler, "Unpassivated AlGaN-GaN HEMTs with minimal RF dispersion grown by plasma-assisted MBE on semi-insulating 6H-SiC substrates," *IEEE Electron Device Lett.*, vol. 24, pp. 57–59, Jan. 2003.

[8] R. Behtash, H. Tobler, M. Neuburger, A. Schurr, H. Leier, Y. Cordier, F. Semond, F. Natali, and J. Massies, "AlGaN–GaN HEMTs on Si(111) with 6.6 W/mm output power density," *Electron. Lett.*, vol. 39, pp. 626–628, 2003.

[9] S. J. Heikman, S. Keller, S. P. DenBaars, and U. K. Mishra, "Growth of Fe-doped semi-insulating GaN by metalorganic chemical vapor deposition," *Appl. Phys. Lett.*, vol. 81, pp. 439–441, 2002.

[10] S. C. Binari, L. B. Rowland, G. Kelner, W. Kruppa, H. B. Dietrich, K. Doverspike, and D. K. Gaskill, "DC, microwave, and high-temperature characteristics of GaN FET structures," in *Proc. Int. Symp. Compound Semicond.*, San Diego, CA, Sept. 18–22, 1994, pp. 459–462.

[11] M. S. Shur and M. A. Khan, "Optoelectronic GaN-based field effect transistors," *Proc. SPIE*, vol. 2397, pp. 294–303, 1995.

[12] A. Chini, J. Wittich, S. J. Heikman, S. Keller, S. P. DenBaars, and U. K. Mishra, "Power and linearity characteristics of GaN MISFETs on sapphire substrate," *IEEE Electron Device Lett.*, vol. 25, pp. 55–57, Jan. 2004.

[13] D. S. Green, J. S. Speck, and U. K. Mishra, "Carbon doping of GaN with CBr_4 in RF plasma-assisted molecular beam epitaxy," J. Appl. Phys., to be published.

[14] M. J. Manfra, N. G. Weimann, J. W. P. Hsu, L. N. Pfeiffer, and K. W. West, "Dislocation and morphology control during molecular-beam epitaxy of AlGaN–GaN heterostructures directly on sapphire substrates," *Appl. Phys. Lett.*, vol. 81, pp. 1456–1458, 2002.

[15] P. Waltereit, C. Poblenz, S. Rajan, U. K. Mishra, and J. S. Speck, "Growth of GaN buffer layers on 4H-SiC(0001) by plasma-assisted molecular-beam epitaxy for high-mobility electron transistors," Appl. Phys. Lett., submitted for publication.

[16] B. Heying, X. H. Wu, S. Keller, Y. Li, D. Kapolnek, B. P. Keller, S. P. DenBaars, and J. S. Speck, "Control of GaN surface morphologies using plasma-assisted molecular-beam epitaxy," *Appl. Phys. Lett.*, vol. 68, pp. 643–645, 1996.